Torsion in Multi-cell Box Beam

Name: Joost Hubbard

Student ID: 210372773

Module Code: EMS609

Module Title Aircraft Structures

Coursework Name: Torsion in Multi-cell Box Beam

Abstract

The ‘Torsion in Multi-cell Box Beam’ coursework was conducted to compare the shear flow and shear centre values found through simulation and hand calculation – an application of the theory covered in the wider EMS609 module. An idealized wing box structure was created in Abaqus, applying schematic dimensions to create a three-dimensional structure which was then put under boundary conditions and a point load. This model was then meshed and converged to ensure accurate values; the in-plane shear stresses (S12) output from this simulation were the used to calculate the required values. The calculated values from simulation were then compared to hand calculations. Significant disparity was found between the two methods, with shear flow errors ranging from 4.08% to 2289.66% between hand calculation and FEM. The shear centre error was smaller, being around 4.06%. Overall, Abaqus (FEM) is more accurate than hand calculation when analysing a complex structure since it avoids human errors and more accurately represents the stresses in the structure.

Table of Contents

Abstract 1
1. Introduction 2
2. FEM Modelling 3
3. Results 5
3.1 Mesh Convergence 5
3.2 Simulation Results 7
3.3 Hand Calculation 8
4. Discussion 9
5. Conclusion 10
6. References 10
7. Appendix 11
7.1 Hand Calculation 11

1. Introduction

The torsion in a multi-cell box beam coursework was conducted to compare shear flow values alongside the shear centre for a multi-cell wing box from two sources – Abaqus simulation and hand calculations. This acted as application of theory covered in the EMS609 module in addition to simulation proficiency.

Within aerospace applications, the wing box is a major structural component from which the wings extend. While the term typically refers to the section of the fuselage between the wing roots, some aircraft designs may consider it to extend beyond this int the main wing body (Immanuvel, 2014). To perform its role, the wing box must provide stability and strength while minimizing weight – a common set of criteria across all aircraft structures (Chintapalli, 2006). This is specifically tur since the wings of an aircraft experience large torsion moments across the duration of a flight – from take-off to cruise to landing. To ensure these requirements are met, torsion calculations are often carried out to ensure that a design is safe for the duration of a typical flight.

The wing box of an aircraft is in essence a thin-walled tubular structure, with interior spar webs creating multiple cells within it. The main components of the structure are the outer skin, the spars, the stringers, and the ribs. A typical wing box structure can be found in figure 1 below.

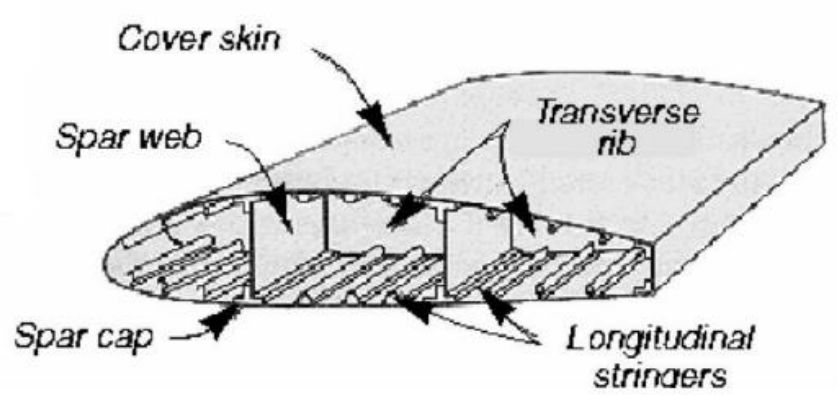

Figure 1 - Typical wing box structure (Toropov, 2023).

In the case of the multi cell box beam coursework a simplified schematic was used was used – in a practice commonly referred to as structural idealization. This model made use of booms and webs to represent the components of the wing box – making the following assumptions (University of Sydney - Faculty of Engineering, 2013):

1. The longitudinal stiffeners and spar flanges carry only axial stresses,
2. The web, skin and spars webs carry only shear stresses,
3. The axial stress is constant over the cross section of each longitudinal stiffener,
4. The shearing stress is uniform through the thickness of the webs,
5. Transverse frames and ribs are rigid within their own planes and have no rigidity normal to their plane.

This results in the schematic shown in figure 2. In this case, the structure has been reduced to just webs and booms. It should also be noted the top and bottom of the structure is symmetrical.

The idealized version of this structure is what will be used for the later calculation and simulation sections of this report.

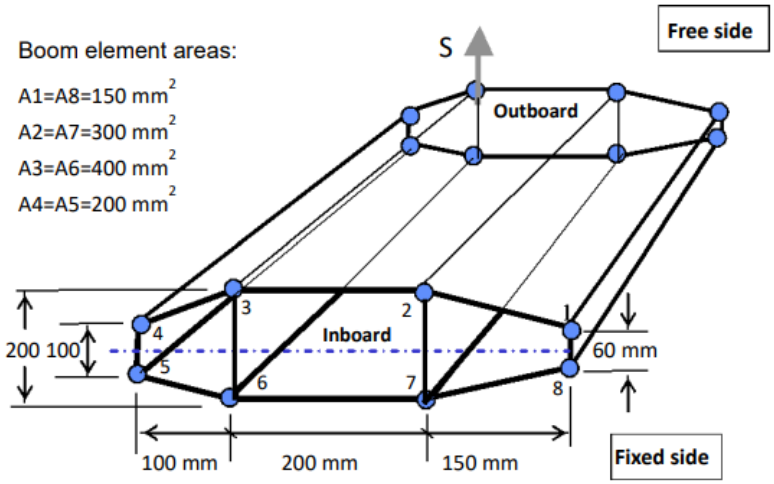

Figure 2 - Idealized wing box structure (Queen Mary University of London, 2024).

2. FEM Modelling

Finite Element Method (FEM) is a computational technique used to analyse structures and predict their behaviour under various forces by dividing them into smaller elements and solving for their responses iteratively (Zienkiewicz, 2005). In this case, FEM was used to model the reaction within the wing box to a point load 'S' to establish the shear flow and centre.

The first step in this process was transferring the idealized wing box schematic into the Abaqus FEM software. Once the sketch was created, it was transferred into a shell to make a three-dimensional model. The dimensions used can be found in figure 2 alongside a beam length of 2000mm. It should be noted that the outboard side of the shell was covered and then partitioned. into six segments, a horizontal partition was added in addition to the 3-6 and 2-7 webs that already portioned the face. The inboard side remained open.

Subsequently, the web sections were created and assigned. To do this, the material of the multi-cell box beam was created inside of Abaqus as given in the handout; the properties were an Youngs modulus 72 GPa and a Poison ratio of 0.28. It should be noted that Youngs modulus was input as 72000 MPa in the Abaqus software to ensure unit consistency.

The web sections were then created making sure to use the shell category and homogenous type. This allowed for the web thicknesses to be input and materials to be assigned. Each web thickness was applied as shown in the table below with each section using the material created prior. Finally, the web sections were applied to their counterparts in model.

Table 1 - Web section thicknesses in mm.

Web Section	Thickness (mm)
1-2	5
2-3	15
3-4	10
4-5	20
5-6	10
6-7	15
7-8	5
8-1	10
3-6	20
2-7	20
Outboard Face	5

Next, the boom sections were created and assigned to the model. The booms in the idealized structure had circular profiles and as such were created using their respective radii – detailed in

table 2. The boom profiles were then applied when creating the beam sections – which was done for all boom sections A1 to A8. To apply the beam sections, stringers were created between the booms with the identical areas (for example A1 and A8), creating 4 in total. The beam sections were then applied to their respective sections in the model.

Table 2 - Boom radii in mm.

Boom Reference	Boom Element Area (mm^2)	Boom Element Radius (mm)
A1 & A8	150	6.91
A2 & A7	300	9.77
A3 & A6	400	11.28
A4 & A5	200	7.98

Next the shell normal were flipped ensure accurate measurements in later simulation. This was done ensuring all shells had the same positive and negative face. The internal shells were aligned to share the same orientation as the 8-1 web.

After this, the beam and material orientations were assigned. The beam orientations were aligned with the positive Z direction in the global coordinate system. The plate orientations were assigned individually using datum coordinate systems, ensuring that the positive Z was normal to the place and the positive X was in line with the plate in a clockwise direction. Figure 3 below outlines the plate coordinate system.

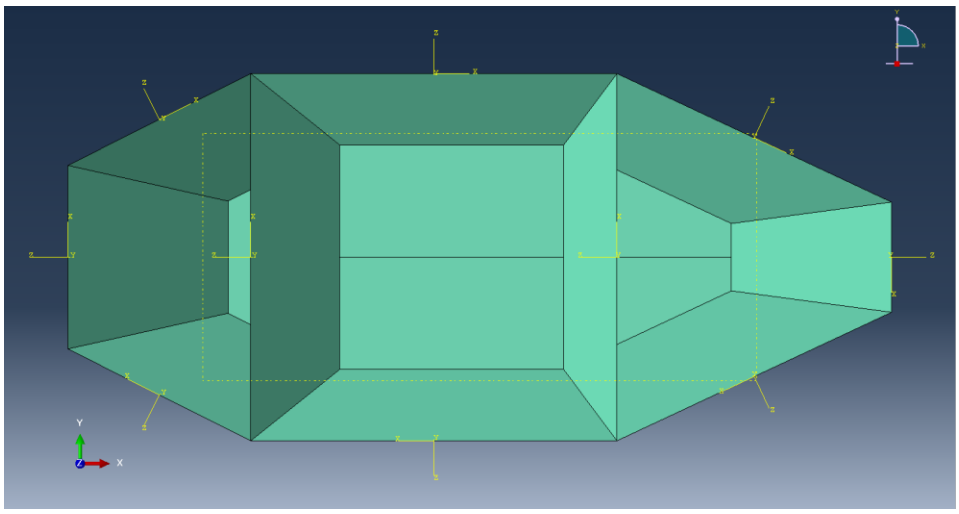

Figure 3 - Inboard face of the model with the plate datum coordinate systems visible.

The next step involved making a new step within Abaqus to facilitate the addition of loads and boundary conditions. The new step was called ‘Loading’ and was ‘static, general’ type. The conditions added were as follows:

1. A point load ‘S’ was added to the outboard point of boom 3 as specified in figure 2. This was applied as a concentrated force in the global coordinate systems positive Y direction using a magnitude of 5000 N.
2. The outboard face was set under a rigid body constraint. This ensured no deformation in the profile of the beam when under load.

3. The inboard face was set under a fixed, encastre constraint. This ensured no displacement or rotation occurred.

Next, the element shape for the whole model was set as a structured quad. This ensured that when the mesh was generated in later steps, every element would be a uniform quadrilateral.

Penultimately, the mesh for the model was generated and the simulation was completed. This meant setting an approximate global element size and then meshing the model before submitting the simulation as a job to complete. The global element size used was 3.5 mm as determined by mesh convergence carried out on the entire model to ensure accurate results. Each induvial plate was then simulated individually to output the in-plane shear stresses (S12) on the upper and lower surfaces of each web.

The shear stress on each web was then determined using the output S12 values. For each web, the upper and lower shell stress was recorded from Abaqus and then both values were averaged to give one value for each web. This value was then divided by the number of elements present in the shell and multiplied by the shell thickness. This gave the final shear flow value for each web.

Finally, the shear centre was determined using Abaqus. This was done through the comparison of y displacement in two distinct loading scenarios. In both cases the load was equal concentrated force equal to load S. The loads were positioned on the outboard side of booms 2 and 3. A path was created across the outboard face as a partition in the x direction, creating two equal halves. The displacement was plotted against the true distance along the face both in mm. The intercept was taken to be the shear centre position.

3. Results

The results section of this report covers the mesh convergence process as well as the requested simulation and calculation results.

3.1 Mesh Convergence

Mesh Convergence is the process by which the appropriate mesh for simulation is determined. A mesh can be taken as converged when there is little change in the solution with additional mesh refinement. In a consistent discretisation of the mesh, the truncation errors start to become more negligible as the width reduces (Müller, 2020). In the case of the multi-cell box, the mesh was repeatedly refined, and the maximum von-misses stress recorded. This allowed for the determination of an appropriate mesh for later use in the simulation of the in-plane stresses in each plate. Images of the mesh convergence alongside tabular and graphical representation of results are displayed below.

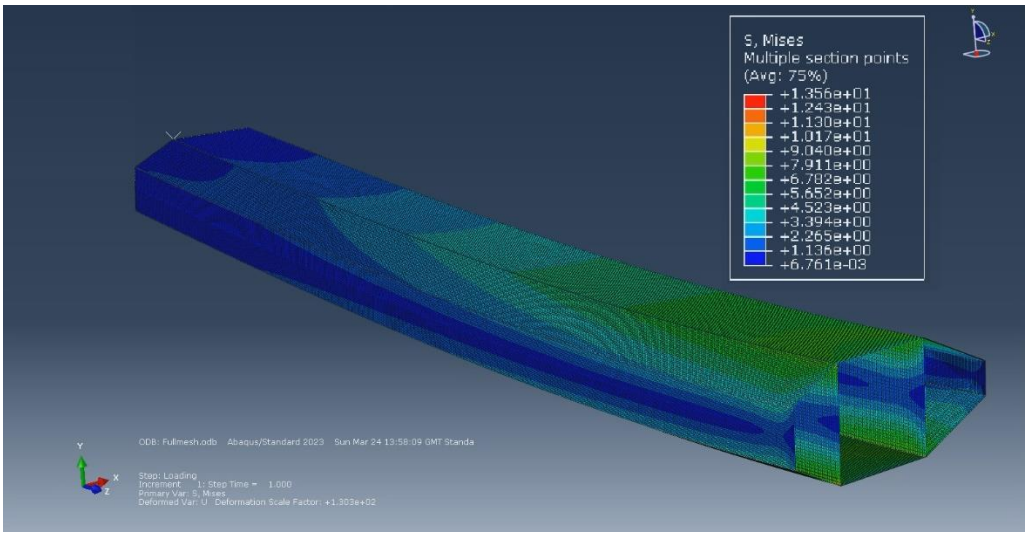

Figure 4 – Converged mesh displaying Von Misses Stress (in N/mm) across the whole multi-cell box.

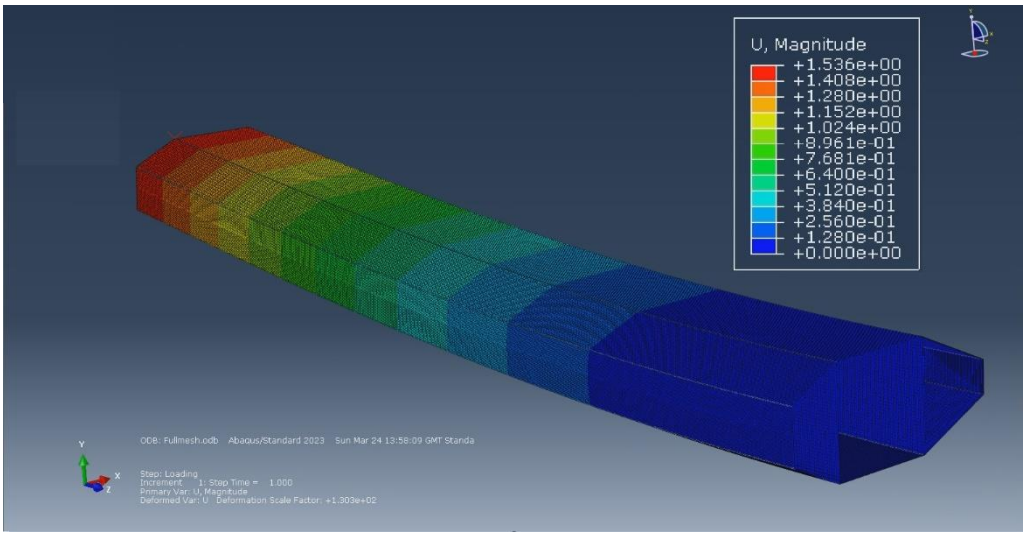

Figure 5 - Converged mesh displaying displacement (in mm) across the whole multi-cell box.

Table 3 - Mesh convergence data.

Element size (mm)	No. of elements	Max V. Misses Stress (N/mm)
20	7344	1.13E+01
15	13313	11.8158
10	29376	12.4389
5	116725	13.2586
4	180565	13.4544
3.5	242494	13.5564

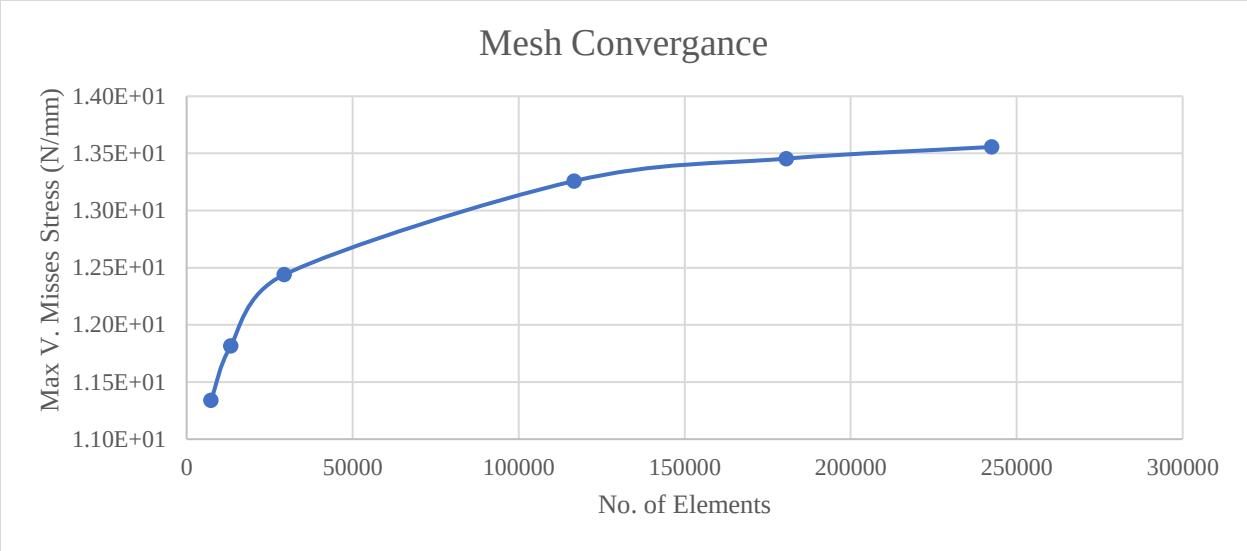

Graph 1 – Mesh convergence graph for the multi-cell box beam. Max Von Misses Stress (in N/mm) is plotted against the number of elements.

The mesh convergence graph demonstrates the effect of mesh refinement on the solutions reached through Abaqus simulation. As the element size reduces, the mesh becomes more refined, leading to convergence on the true solution. It can be seen from graph 1, that increasing element size displays logarithmic growth – initial rapid growth followed by decreasing growth and a plateau. This is reflected in table 3, where the Von Misses stress converges on a value of 13.55 N/mm at a global element size of 3.5 mm with 242494 elements. Since it had converged, this was the same element size used for the later simulations run in Abaqus. It should be note that mesh refinement could not be continued due element limits on the student licence.

3.2 Simulation Results

The shear flow values associated with each web was calculated. This was done using the values shown in table 4 resulting in the shear flow for each web in N/mm.

Table 4 - Abaqus shear flow calculations.

Field Output	No. of elements	Thickness (mm)	Top of shell stress (N/mm^2)	Bottom of shell stress (N/mm^2)	Average stress (N/mm^2)	AVG/Elements (N/mm^2)	Shear flow (N/mm)
Web 1-2	26837	5	-76.2372	-492.6	-284.4186	-0.010598003	-0.053
Web 2-3	32547	15	8.37E+03	6.85E+03	7606.115	0.233696347	3.5054
Web3-4	17130	10	8.89E+03	8.35E+03	8619.395	0.503175423	5.0318
Web 4-5	21127	20	9.13E+03	7.86E+03	8492.77	0.401986557	8.0397
Web 5-6	17130	10	8.89E+03	8.35E+03	8619.395	0.503175423	5.0318
Web 6-7	32547	15	8.37E+03	6.85E+03	7606.115	0.233696347	3.5054
Web 7-8	26837	5	-76.213	-492.622	-284.4175	-0.010597962	-0.053
Web 8-1	21127	10	-3.10E+03	-2.46E+03	-2777.74	-0.131478203	-1.315
Web 3-6	21127	20	-1.05E+04	-1.18E+04	-11138.15	-0.527199792	-10.54
Web 2-7	21127	20	-7.05E+03	-8.34E+03	-7696.01	-0.364273678	-7.285

The shear centre was determined using the method covered in section 2, using the y displacement plots for two different loading conditions. The graph plotted (graph 2) is shown below with an

intercept of at a true distance along path of 271.26. This value can be taken to be the distance in mm into the outboard face from the 8-1 web – as indicated in figure 6.

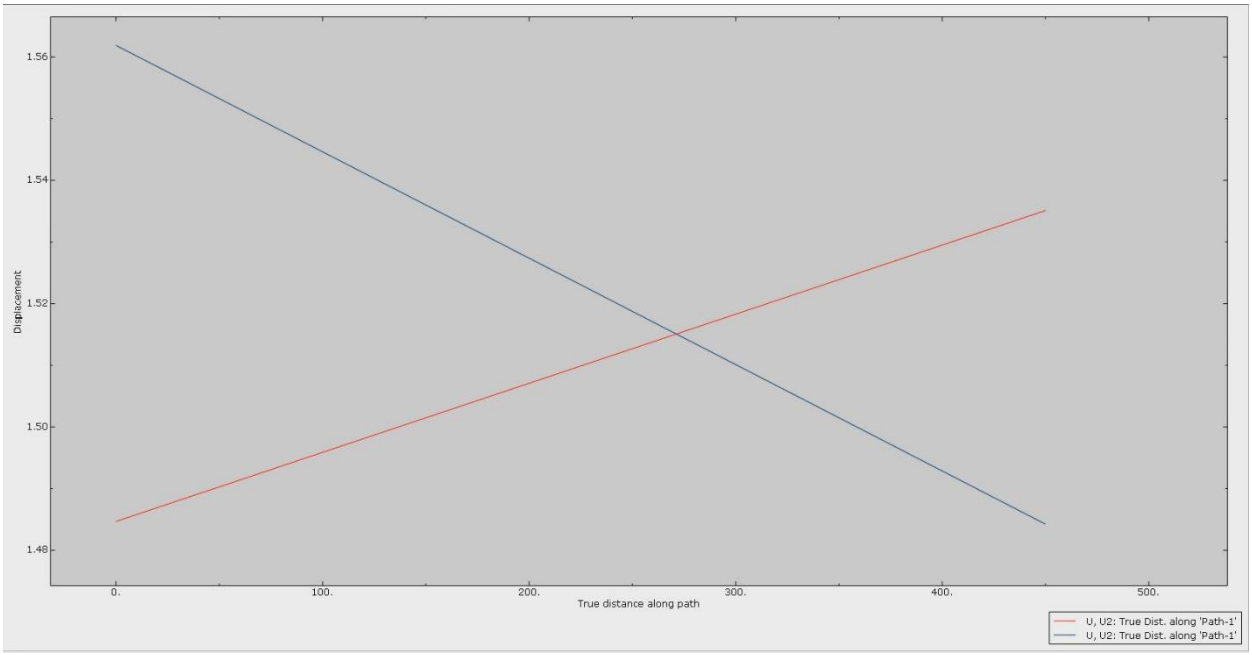

Graph 2 - Y displacement with distance along the outboard face of the structure. The red and blue lines indicate two equal magnitude loading conditions located at the end of booms 2 and 3 on the outboard face.

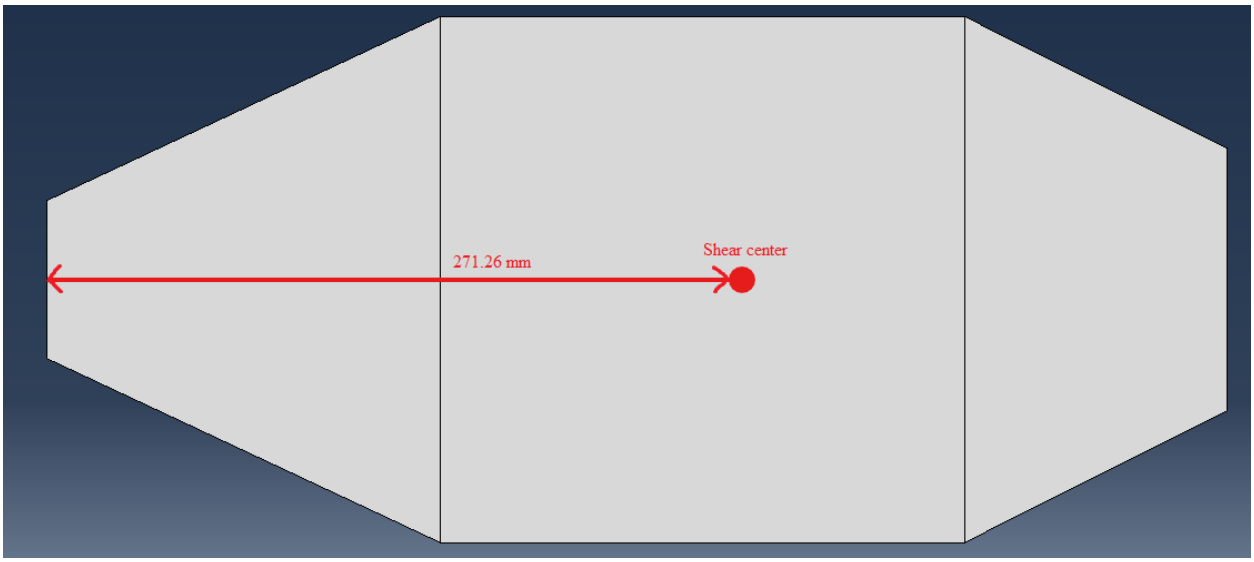

Figure 6 - Location of the shear centre on the outboard face.

3.3 Hand Calculation

The hand calculation was completed to give the shear flow in each web alongside the shear centre. The method used to complete this is covered fully in the appendix. The results for all hand calculation, in addition to percentage difference to the Abaqus values, can be seen below in table 5.

Table 5 – Non-reoriented hand calculation shear flow values.

Web	Shear Flow (N/mm)	Percentage Difference to Abaqus
q12	1.160	2289.66%
q23	0.469	86.63%
q34	-2.517	150.01%
q45	-5.791	172.03%
q56	-2.517	150.01%
q67	0.469	86.63%
q78	1.160	2289.67%
q81	2.634	300.32%
q36	-10.112	4.09%
q27	9.132	225.34%

Making sure to analyse the orientations used for the hand calculation (shown in figure 7), table 5 can be transformed into table 6. Thes are the final values associated with hand calculation shear flow.

Table 6 - Reoriented hand calculation shear flow values.

Web	Shear Flow (N/mm)	Percentage Difference to Abaqus
q12	-1.160	2089.66%
q23	0.469	86.63%
q34	2.517	49.99%
q45	5.791	27.97%
q56	2.517	49.99%
q67	0.469	86.63%
q78	-1.160	2089.67%
q81	-2.634	100.32%
q36	-10.112	4.09%
q27	-9.132	25.34%

The method for the calculation of the shear centre associated with hand calculations is again displayed in the appendix. The shear centre is calculated to be 167.49 mm from the 4-5 web. For the sake of comparison, this means the shear centre is located 282.51mm from the 8-1 web.

4. Discussion

Through the completion of both the Abaqus simulation and hand calculations, values for the shear flow in each web as well as the shear centre were found.

Prior to the determination of any values, mesh convergence was completed for the multi-cell box beam. This resulted in a converged Von-Misses stress value of 13.36 N/mm with a global element size of 3.5mm and 242494 elements. The shear flow values calculated from Abaqus simulation appear to be of a reasonable values (shown in table 4) and the shear centre is calculated to be 271.26 mm into the structure from the 8-1 web (shown in figure 6). It is worth

nothing that purely from an accessibility standpoint, the Abaqus process of determining the shear flow and centre required less hands-on mathematics and as such provided less opportunity for human miscalculation.

The hand calculation values were determined through the calculations covered in the appendix section of this report. Table 5 displays the shear flow values calculated in this manner. The shear centre can is determined to be 282.51mm from the 8-1 web.

Comparison of the Abaqus and hand calculated shear flow values provides insight into validity. The large range of accuracy across the hand calculation shear flows is obvious, with errors ranging from as large as 2289.66% and as small as 4.09%. The shear percentage difference in shear centre is found to be 4.06% between Abaqus and the hand calculation methods.

The inconsistent errors with the shear flow values across the body can be attributed to the myriad of assumptions made during the hand analysis of the swing box. One example of this is the assumption that the webs only carry shear stresses, an assumption not made in the Abaqus simulation and as such leading to inaccuracy. This is reflected in the smaller error values associated with non-inclined webs, since these webs would only be experiencing shear forces. The smaller error associated with the shear flow location is also indicative of this. Another reason for the disparity could be that of human error within the hand calculation – a result of the complex geometry of the multicell beam.

To improve the accuracy of the finite element modelling, steps could be taken to improve the element size and shape. The limits on the student edition of Abaqus restricted any further mesh refinement past 250000 elements while the only element type tested quadrilateral. Taking steps such as mesh refinement or varied element geometry could improve accuracy across the simulation.

5. Conclusion

By completion of the ‘Torsion in Multi-cell Box Beam’ coursework, Abaqus and hand calculation methods were used to find shear flow and centre values which were then compared. Significant disparity was found between the two methods, with shear flow errors ranging from 4.08% to 2289.66%. The shear centre error was smaller, being around 4.06%. Due to the complexity of the multi-cell beam the Abaqus finite element simulation is more likely to be accurate due to the removal of human error within calculation. In addition to this, it is clear while structural idealisation can lead to varied inaccuracy in shear flow, the calculation of the shear centre is mostly unaffected. To improve the accuracy of further simulation, finite element modelling should be used – perhaps with more testing on varied mesh refinement and element geometry.

6. References

1. Chintapalli, S., 2006. *Preliminary structural design optimization of an aircraft wing-box,* s.l.: Concordia University.

2. Immanuvel, D. A. K. M. P. a. S. S., 2014. Stress analysis and weight optimization of a wing box structure subjected to flight loads.. *The International Journal Of Engineering And Science (IJES),* 3(1), pp. pp.33-40.

3. Müller, J.-D., 2020. *Essentials of Computational Fluid Dynamics.* s.l.:Boca Raton: CRC Press..

4. Queen Mary University of London, 2024. *Torsion in Multi-cell Box Beam Coursework Specification.* London: s.n.

5. Toropov, P. V., 2023. *Aerospace Structures: shear of closed section beam lecture notes.* London: Queen Mary University of London.

6. University of Sydney - Faculty of Engineering, 2013. *Structures Part 6 - Structural Idealisation.* [Online]
Available at: https://www.aeromech.usyd.edu.au/structures/acs1-p61.html
[Accessed 23 03 2024].

7. Zienkiewicz, O. T. R. a. Z. J., 2005. *The finite element method: its basis and fundamentals.* 6th ed. Swansea: Elsevier.

7. Appendix

The appendix covers equations and calculations not relevant for data analysis in the report.

7.1 Hand Calculation

This section details the hand steps taken to complete hand calculation with the equations used.

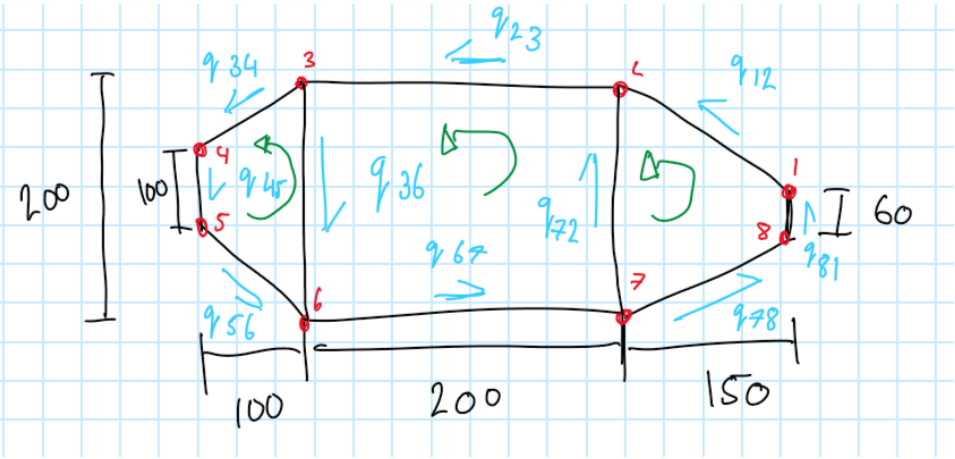

Figure 7 - Drawing dictating orientations used for hand calculations.

Initially, the second moment of area was found for the beam section. This was done using equation 1.

$$I_{xx} = \sum_{i=1}^{n} A_i y_i^2 \quad [1]$$

$$I_{xx} = 2[(200 \times 50\text{^}2\ ) + (400 \times 100\text{^}2\ ) + (300 \times 100\text{^}2\ ) + (150 \times 30\text{^}2\ )] = 1.527 \times 10^7\ mm^4$$

Next, since the wing box is symmetrical about its x-axis, the following shear flow (q) equalities were identified.

$$q_{12} = q_{78} \qquad q_1 = q_{12}$$

$$q_{23} = q_{67} \qquad q_2 = q_{23}$$

$$q_{34} = q_{56} \qquad q_3 = q_{34}$$

Next, of each of the symmetrical boom pairs was crossed, creating shear flow equations for each. This made use of equation 2 and the previous identities.

$$\boldsymbol{q_{n+1} = q_n - \frac{V_y}{I_{xx}}(\sum_{i=1}^{n} A_i y_i\ )]} \qquad [\mathbf{2}]$$

Crossing Boom 1: $q_{81} = q_1 + \frac{750}{509}$

Crossing Boom 2: $q_{27} = q_2 - q_1 + \frac{5000}{509}$

Crossing Boom 3: $q_{36} = q_2 - q_3 - 13.09757695$

Crossing Boom 4: $q_{45} = q_3 - \frac{5000}{1527}$

Next, the torsion moment around the point of loading was solved making use of equation 3 and the previously created shear flow equations. It should be noted that the fourth term is negative as per the negative shear flow in the

$$\boldsymbol{M_0^q = \sum q_i A_{area}} \quad [\mathbf{3}]$$

$$M_0^q = 0 = \left(2(5000)\left(q_3 - \frac{5000}{1527}\right)\right) + \left(2(10000q_3)\right) + \left(2(20000q_2)\right) + \left(2(20000)\left(q_2 - q_1 + \frac{5000}{509}\right)\right) + \left(2(22000q_1)\right) + \left(2(10500)\left(q_1 + \frac{750}{509}\right)\right) + \left(2(7000q_1)\right)$$

$$M_0^q = 0 = 30000q_3 + 80000q_2 + 79000q_1 - 391126.3916$$

Next, the twist angle equations are created using equation 4 and then equated.

$$\boldsymbol{\left.\frac{\theta}{L}\right|_n = \frac{1}{2AG}\oint \frac{q_i s_i}{t} ds} \quad [\mathbf{4}]$$

$$\left.\frac{\theta}{L}\right|_1 = \frac{1}{2(15000)}[43.2842q_3 - 10q_2 + 114.6037197119]$$

$$\left.\frac{\theta}{L}\right|_2 = \frac{1}{2(40000)}\left[-10q_3 + \frac{140}{3}q_2 - 10q_1 - 32.74394239\right]$$

$$\left.\frac{\theta}{L}\right|_3 = \frac{1}{2(19500)}\left[-10q_2 + 82.2116q_1 - \frac{45500}{509}\right]$$

$$\left.\frac{\theta}{L}\right|_1 = \left.\frac{\theta}{L}\right|_2 = -4.2842q_3 + \frac{55}{2}q_2 - \frac{15}{4}q_1 - 126.9027767$$

$$\left.\frac{\theta}{L}\right|_2 = \left.\frac{\theta}{L}\right|_3 = 10q_3 - \frac{2620}{39}q_2 + 178.6391795q_1 - 150.6221349$$

Next, the combined twist angle equations are solved simultaneously with the torsion moment equation to give values of q_1, $q_2$and q_3.

q_1 = 1.1603 q_2 = 0.4687 q_3 = -2.51657

Next, the solved q values are substituted back into the shear flow equations to give values for each shear flow.

$q_{12} = q_{78} = q_1 = 1.16\ N/mm$

$q_{23} = q_{67} = q_2 = 0.469\ N/mm$

$q_{34} = q_{56} = q_3 = -2.517\ N/mm$

$q_{81} = q_1 + \frac{750}{509} = 2.634\ N/mm$

$q_{27} = q_2 - q_1 + \frac{5000}{509} = 9.132\ N/mm$

$q_{36} = q_2 - q_3 - 13.09757695 = -10.112\ N/mm$

$q_{45} = q_3 - \frac{5000}{1527} = -5.791\ N/mm$

Finally, the shear flow must be calculated. This is done by balancing the moment equation cantered around boom 3 from before with the applied load.

$$5000N \times distance = 30000q_3 + 80000q_2 + 79000q_1 - 391126.3916$$

$$5000N \times distance = 30000(-2.51657) + 80000(0.4687) + 79000(1.1603) - 391126.3916$$

This gives the distance between boom 3 and the shear centre to be 67.49mm. The distance between web 4-5 is thus 100mm + 67.49mm = 167.49mm. From web 8-1 the shear centre is 282.51mm.